A dose-escalation and safety study of gene therapy for CMT4C neuropathy

Elena Georgiou[1], Alexia Kagiava[1], Andreas Hentschel[2], Irene Sargiannidou[1], Revekka Papacharalampous[3,9], Marina Stavrou[1], Christina Tryfonos[4], Jan Richter[4], Andreas Roos[5,6,7,8] and Kleopas A. Kleopa[1,9]

[1]Neuroscience Department, The Cyprus Institute of Neurology and Genetics, Nicosia, Cyprus 2371;

[2]Leibniz-Institut für Analytischen Wissenschaften -ISAS- e.V., Dortmund, Germany [3]Neuropathology Laboratory, The Cyprus Institute of Neurology and Genetics, Nicosia, Cyprus 2371;

[4]Molecular Virology Department, The Cyprus Institute of Neurology and Genetics, Nicosia, Cyprus 2371;

[5]Department of Pediatric Neurology, Centre for Neuromuscular Disorders, University Duisburg- Essen, Essen, Germany.

[6]Department of Neurology, Medical Faculty and University Hospital Düsseldorf, Heinrich Heine University Duesseldorf, Duesseldorf, Germany.

[7]Department of Neurology, Heimer Institute for Muscle Research, University Hospital Bergmannsheil, Ruhr-University Bochum, Bochum, Germany.

[8]Children's Hospital of Eastern Ontario Research Institute, University of Ottawa, Ottawa, Canada.

[9]Center for Neuromuscular Disorders, The Cyprus Institute of Neurology and Genetics, Nicosia, Cyprus 2371

DETAILED MATERIALS AND METHODS

Viral vector production

The production of the mock (AAV9-*hMPZmini.EGFP*) and therapeutic (AAV9-*hMPZmini.SH3TC2.SV40pA*) viral vectors was performed at Virovek CoA. Vectors were produced in insect Sf9 cells by infection with rBV– inCap9-inRep-kozak-hr2 (V289) and either rBV-*hMPZmini.EGFP* (NRG36) for the mock, or rBV-AAV9-*hMPZmini.SH3TC2.SV40pA* for the therapeutic vector. Vectors were purified through 2 rounds of CsCl ultracentrifugations. The CsCl was removed through buffer exchange with 2 PD-10 desalting columns. The final AAV vector product was buffer-exchanged to PBS plus 0.001% pluronic F-68 buffer.

Experimental mice

The intrathecal gene delivery experiments were conducted using wild type (WT) C57BL/6 or *Sh3tc2*$^{-/-}$ mice. The generation and characterization of the *Sh3tc2*$^{-/-}$ mouse model has been described previously (16, 32). All animals were kept under specific pathogen free (SPF), standard controlled conditions of temperature (21–23◦C), humidity, air exchange and light cycle (12/12 h light/dark) and provided with standardized mouse diet and drinking water ad libitum.

Determination of vector genome copy numbers (VGCNs)

To assess vector biodistribution, genomic DNA was extracted from different PNS tissues (i.e., lumbar roots, proximal and distal sciatic nerves, and femoral motor nerves) of mice 6 or 8 weeks after intrathecal vector delivery using the MagPurix Tissue DNA Extraction Kit (Zinexts Life Science. The extracted DNA was analyzed for yield and purity using a Nanodrop 1000 spectrophotometer. 5 µl of DNA was used as template for a duplex digital droplet PCR assay targeting either the EGFP or SH3TC2 gene of the transgene cassette and in parallel TFRC as a reference gene. Following droplet generation on a Bio-Rad QX200 AutoDG ddPCR system (Biorad, France), the emulsion was transferred to a PCR plate and cycled using the following thermal cycler conditions: predenaturation at 95 °C for 5 min, 40 cycles at 95 °C for 30 s, 60 °C for 1 min, and 4 °C for 5 min, and a final step at 60 °C for 10 min. Data acquisition and analysis were performed on a QX200 Droplet Reader and QuantaSoft Software (Biorad, France). The vector genome copy number (VGCN) was calculated from absolute ddPCR quantification as a ratio of the number of target copies to half the number of reference host genome copies.

Tissue processing and expression analysis

For immunofluorescence staining mice were anaesthetized with avertin according to institutionally approved protocols, and then transcardially perfused with phosphate-buffered saline (PBS) followed by fresh 4% paraformaldehyde (Merck, New Jersey, USA) in 0.1M PB buffer. The lumbar spinal cord with all roots attached

as well as sciatic nerves were dissected and frozen for cryosections. Sections were permeabilized in cold acetone and incubated at room temperature with a blocking solution of 5% bovine serum albumin (BSA) (Sigma-Aldrich, Missouri, USA) containing 0.5% TritonTM 561 X (Sigma-Aldrich, Missouri, USA) for 1 h. Rabbit polyclonal primary antibodies against SH3TC2 (1:100; Abcam, Cambridge, UK), or EGFP (1:1000; Invitrogen, Massachusetts, USA) were incubated at 4°C overnight. Slides were then washed in PBS and incubated with anti-rabbit fluorescein (FITC)-conjugated (1:1000; Jackson ImmunoResearch, 111-486-003) or with anti-rabbit cross-affinity purified rhodamine-conjugated (1:3000; Jackson ImmunoResearch, 111-026-003) secondary antibodies. Slides were mounted with fluorescent mounting medium (DAKO) and images photographed under a fluorescence microscope (Nikon Eclipse Ni) with a digital camera (DS-Qi2) using NIS-Elements software. Quantification of reporter gene EGFP (mock vector) or SH3TC2 (full vector) expression was performed at 6 weeks post-injection in ventral lumbar spinal root sections and in sciatic nerve teased fibres (n=3 mice) in images taken from five different areas in each slide. The number of EGFP- or SH3TC2-positive Schwann cells as well as the total number of cells in each picture was counted to determine the average expression ratio.

Hematoxylin and Eosin staining

Tissue sections embedded in paraffin were stained with Harris's haematoxylin (freshly filtered) for 3 minutes, followed by washing with distilled water and staining with aqueous eosin for 6 minutes. Afterwards they were dehydrated in ascending concentrations of alcohol and cleared in xylene (70%, 95%, 100% x 2 and xylene x 3). Finally, the tissue slides were mounted with DPX.

2.5 Motor behavioral testing

2.5.1 Rotarod analysis: Each animal was placed daily for one week on a 3.5 cm diameter rod. The initial rod speed was 4 rpm and then accelerating every 30 sec. The time it took for the animal to fall off was recorded. Mice were trained by performing three trials on each of three consecutive days prior to testing. Mice were placed on the rod, and the speed was gradually increased from 4 to 40 rotations per minute (rpm). The trial lasted until the mouse fell from the rod or until the mouse remained on the rod for 600 sec. Testing was performed on the fourth day using two different speeds, 20 and 32 rpm. The latency to fall was calculated for each speed.

2.5.2 Grip strength test: We focused only on hind limb strength based on our treatment level. Mice were held by the neck’s skin and lowered towards the apparatus (Ugo Basile) until they grabbed a grid with both hind limbs. Mice were gently pulled forward until they released their grip from the grid. Each session

consisted of five consecutive trials. The equipment automatically measures the grams of force required to pry the mouse from the grid.

2.6 Electrophysiological evaluation

Bilateral sciatic nerves were stimulated in anaesthetized animals (n=10 per treatment group) at the sciatic notch and distally at the knee via bipolar electrodes with supramaximal square-wave pulses (5 V) of 0.05 ms. The latencies compound muscle action potentials (CMAP) were recorded by a bipolar electrode inserted between digits 2 and 3 of the hind paw and latencies were measured from the stimulus artefact to the onset of the negative M-wave deflection. Motor nerve conduction velocities (MNCV) were calculated by dividing the distance between the stimulating and recording electrodes by the result of subtracting the distal latency from the proximal latency.

Statistical analysis

The percentage of EGFP or SH3TC2-positive Schwann cells in immunostained lumbar roots and sciatic nerves of WT and Sh3tc2$^{-/-}$mice injected with the mock or full vector, respectively, were compared with Student's t-test. For proteomics data statistical significance was calculated using a Student's t-test in MS Excel. Behavioural testing results, electrophysiological results, and morphological analysis data obtained from mock and fully treated groups were compared with the

Mann-Whitney *U* test (significance level for all comparisons, $P < 0.05$). Each set of data is presented as the mean ± SEM. All statistical analyses were performed using Graph Pad Prism, version 6 (GraphPad Software).

SUPPLEMENTARY FIGURES

Fig. S1.

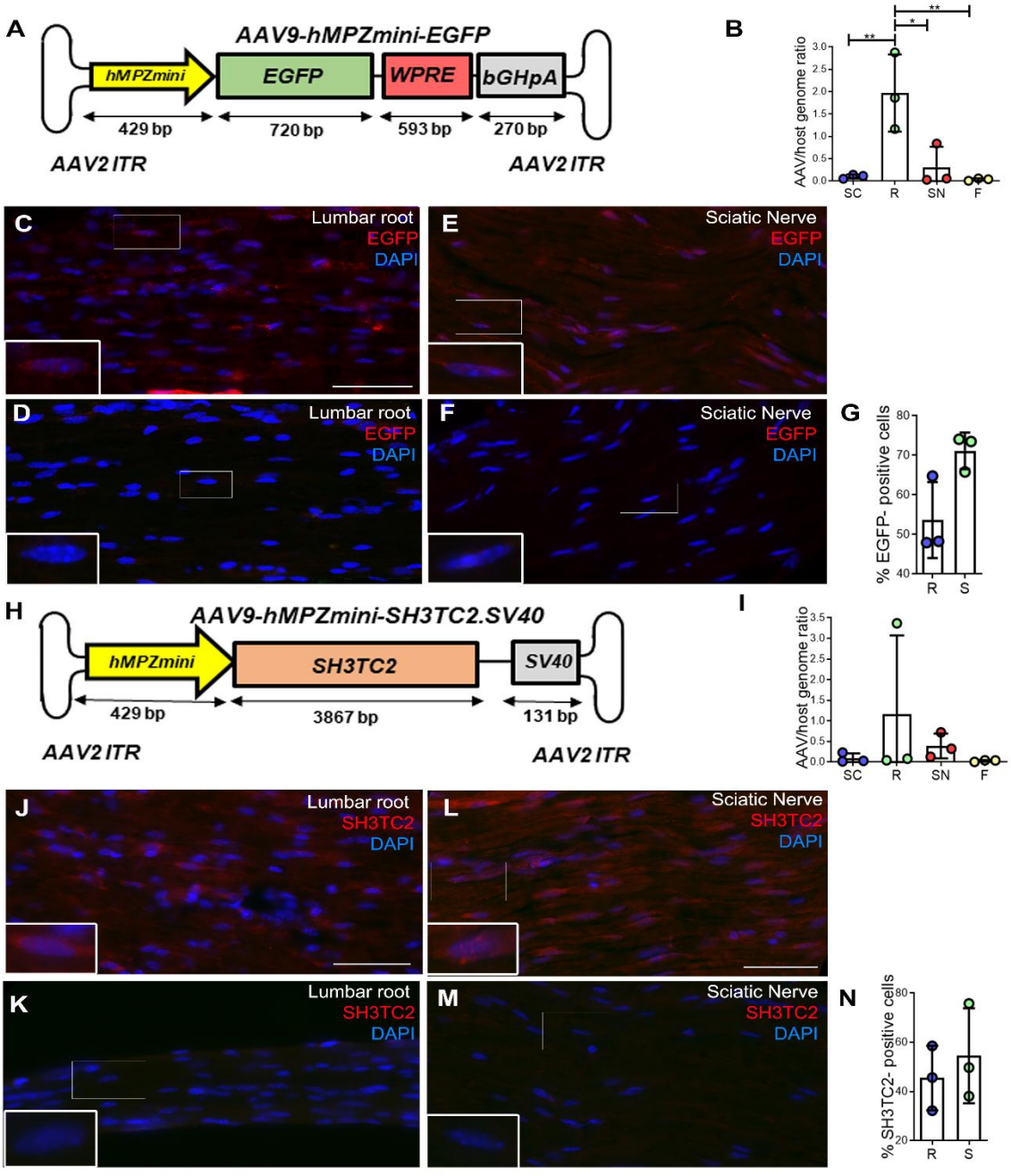

Fig. S1: Cloning and validation of a human minimal *MPZ* promoter and cloning and expression of the therapeutic vector AAV9-*hMPZmini.SH3TC2.SV40pA*. A: Generation of the AAV9-*hMPZmini.EGFP* vector (mock vector driving reporter gene expression) through cloning of the 429 bp distal fragment of the full-length human myelin protein zero (*MPZ*) promoter (*hMPZmini*) upstream of the EGFP coding sequence. **B:** Biodistribution of the AAV9-*hMPZmini.EGFP* vector in spinal cord (SC) and PNS tissues including lumbar spinal roots (R), sciatic nerves (S) and femoral nerves (F) of wild type (WT) mice 6 weeks following lumbar intrathecal injection (vector genome copy numbers represent the ratio of vector to host diploid genome in each tissue). **C-F:** Expression of EGFP in Schwann cells in lumbar roots (**C**) and sciatic nerve sections (**E**) following intrathecal injection of the AAV9-*hMPZmini.EGFP* vector. EGFP shows the characteristic perinuclear cytoplasmic immunoreactivity in most myelinating Schwann cells, while EGFP expression is absent from the corresponding tissues of non-injected control mice (**D** and **F**). **G:** Quantification of expression rates (% EGFP-positive cells) in bilateral sciatic nerves and lumbar spinal roots from n=3 injected mice shows. **H:** Cloning of the AAV9-*hMPZmini.SH3TC2.SV40pA* vector for expression of the human *SH3TC2* gene under the control of *hMPZmini* promoter with replacement of the bGHpA (270 bp) by a SV40pA (131 bp) sequence to a final total size of 4771 bp from ITR to ITR. **I:** Biodistribution analysis of AAV9-*hMPZmini.SH3TC2.SV40pA* in spinal cord (SC) and PNS tissues including lumbar spinal roots (R), sciatic nerves (S) and femoral nerves (F) of *Sh3tc2*$^{-/-}$ mice 6 weeks following lumbar intrathecal injection. **J-M:** Analysis of SH3TC2 expression in lumbar roots (**J**), sciatic nerve sections (**L**), of injected *Sh3tc2*$^{-/-}$

mice shows the characteristic granular perinuclear cytoplasmic immunoreactivity of SH3TC2 in myelinating Schwann cells, while SH3TC2 expression is absent from the corresponding tissues of non-injected littermate mice (**K** and **M**). **N:** Quantification of expression rates (% SH3TC2-expressing cells) in bilateral sciatic nerves and lumbar spinal roots from n=5 mice. Values represent mean ± SEM (One-way ANOVA with Tukey's multiple comparison test, *: p<0.05; **:p<0.01, ***:p<0.001). Scale bars: 20 mm.

Fig. S2.

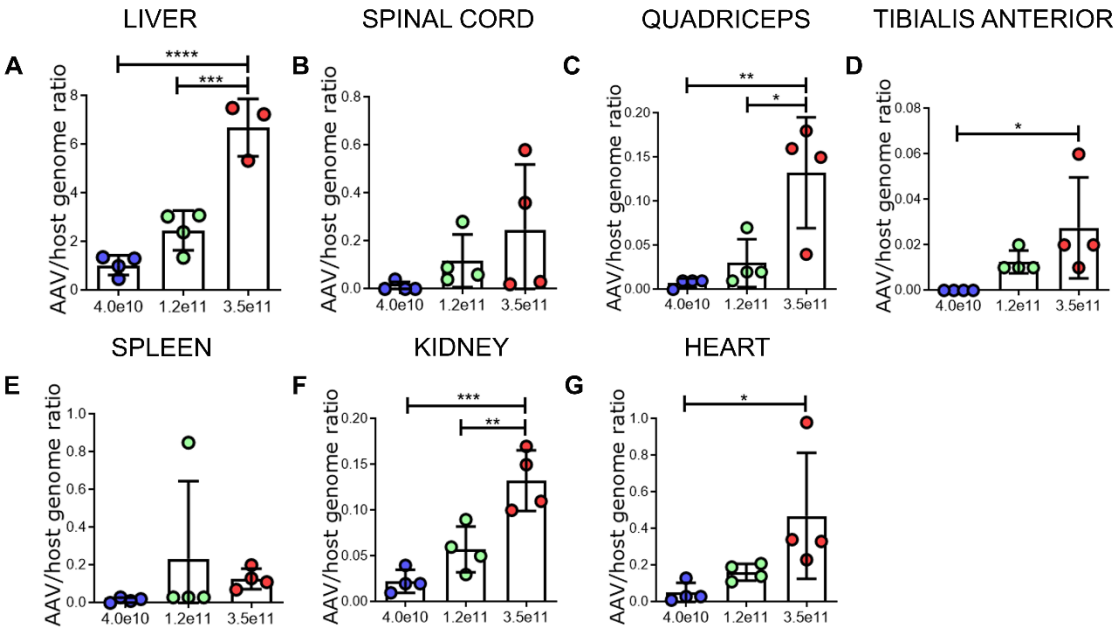

Fig.S2: Systemic vector biodistribution. Biodistribution of AAV9-*hMPZmini.SH3TC2.SV40pA* vector at low, mid, or high dose, as indicated, in spinal cord and peripheral organs 8 weeks after lumbar intrathecal injection into *Sh3tc2*$^{-/-}$ mice.

Quantification of vector genome copy number (VGCN) confirms a dose-dependent biodistribution of AAV9 in most peripheral organs including the liver (**A**), the quadriceps (**C**) and tibialis anterior muscles (**D**), the spleen (**E**), the kidney (**F**) and the heart (**G**), in addition to the spinal cord (**B**). The low dose achieves only a very low biodistribution to peripheral organs, while the high dose achieves the highest biodistribution in most tissues. Values represent mean ± S.D. (*: p<0.05; **:p<0.01, ***:p<0.001; n=4 mice per group).

Fig.S3

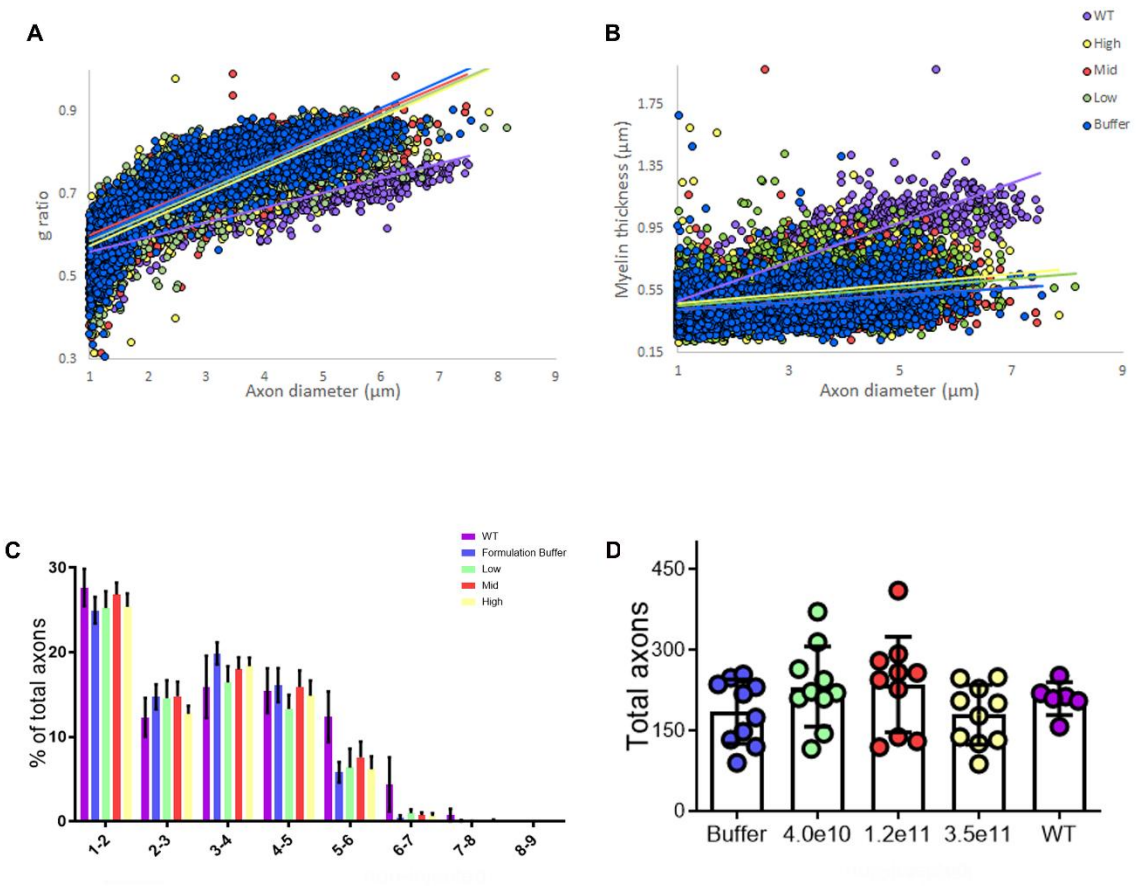

Fig. S3. **Axonal profiles in anterior lumbar roots**. Scatterplots displaying as indicated g-ratios (A) and myelin thickness (B) of individual axons versus axonal diameter in anterior lumbar roots (blue points: buffer-treatment group; green points: low dose vector-treated group; red points: mid dose vector-treated group; yellow points: high dose vector-treated group; purple points: WT group; each point corresponds to one fibre). There is a dose-dependent shift towards better myelin profiles in treatment groups compared to buffer controls. C: Axon profiling with quantitative analysis of axons diameters. There is a shift towards smaller diameter (<2 µm) fibers in *Sh3tc2*-/- compared to WT mice with partial amelioration of this shift in treated animals. D: The total number of axons does not differ significantly between *Sh3tc2*-/- treatment groups and WT mice. Values represent mean ± SEM. (1-way ANOVA with Tukey's multiple-comparison test).

Fig.S4

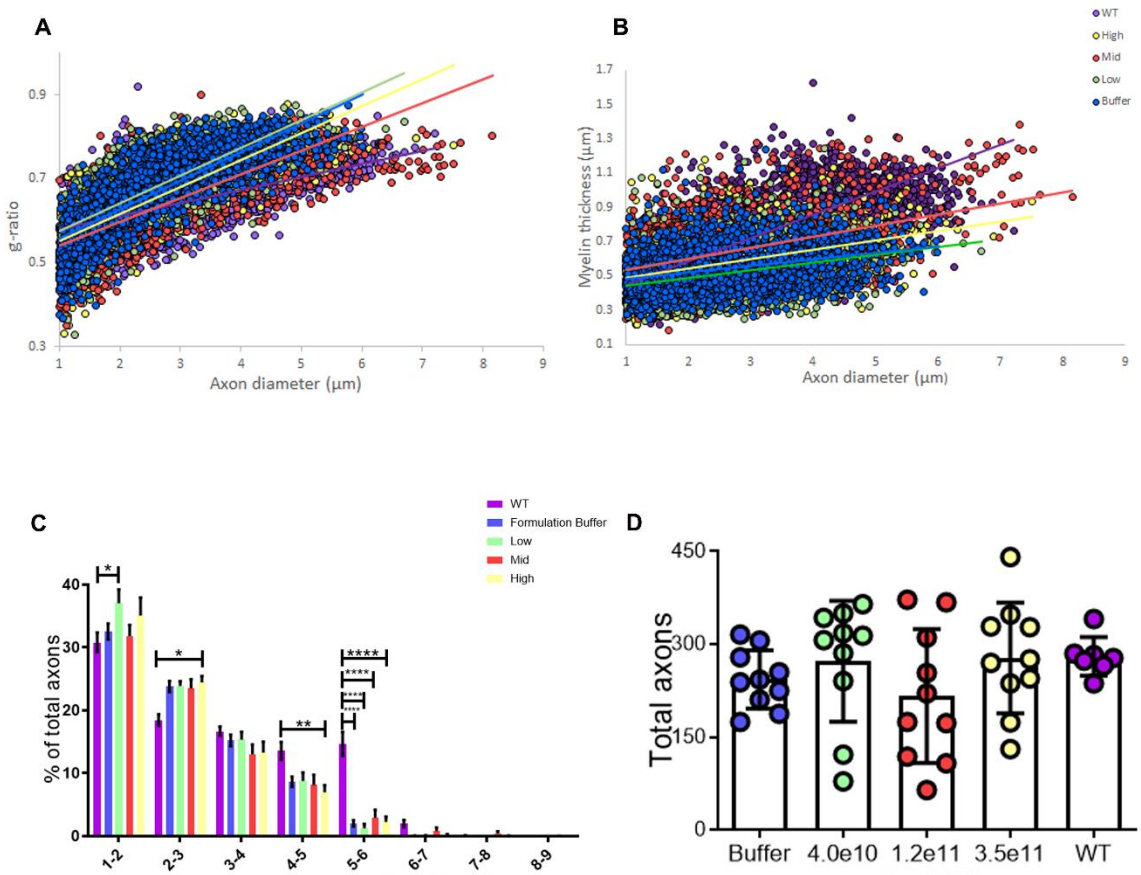

Fig.S4: Axonal profiles in femoral motor nerves. Scatterplots displaying as indicated g-ratios (**A**) and myelin thickness (**B**) of individual axons versus axonal diameter in femoral motor nerves (blue points: buffer-treatment group; green points: low dose vector-treated group; red points: mid dose vector-treated group; yellow points: high dose vector-treated group; purple points: WT group; each point corresponds to one fibre). No significant change in axon profiles is observed in the treatment groups compared to the buffer controls. **C:** Axon profiling with quantitative analysis of axons diameters. There is a shift

towards smaller diameter (<2 μm) fibers in *Sh3tc2*$^{-/-}$ compared to WT mice while no improvement in larger diameter fibers was observed in treated mice. **D:** The total number of axons does not differ significantly between *Sh3tc2*$^{-/-}$ treatment groups and WT mice. Values represent mean ± SEM. (1-way ANOVA with Tukey's multiple-comparison test).

Fig. S5

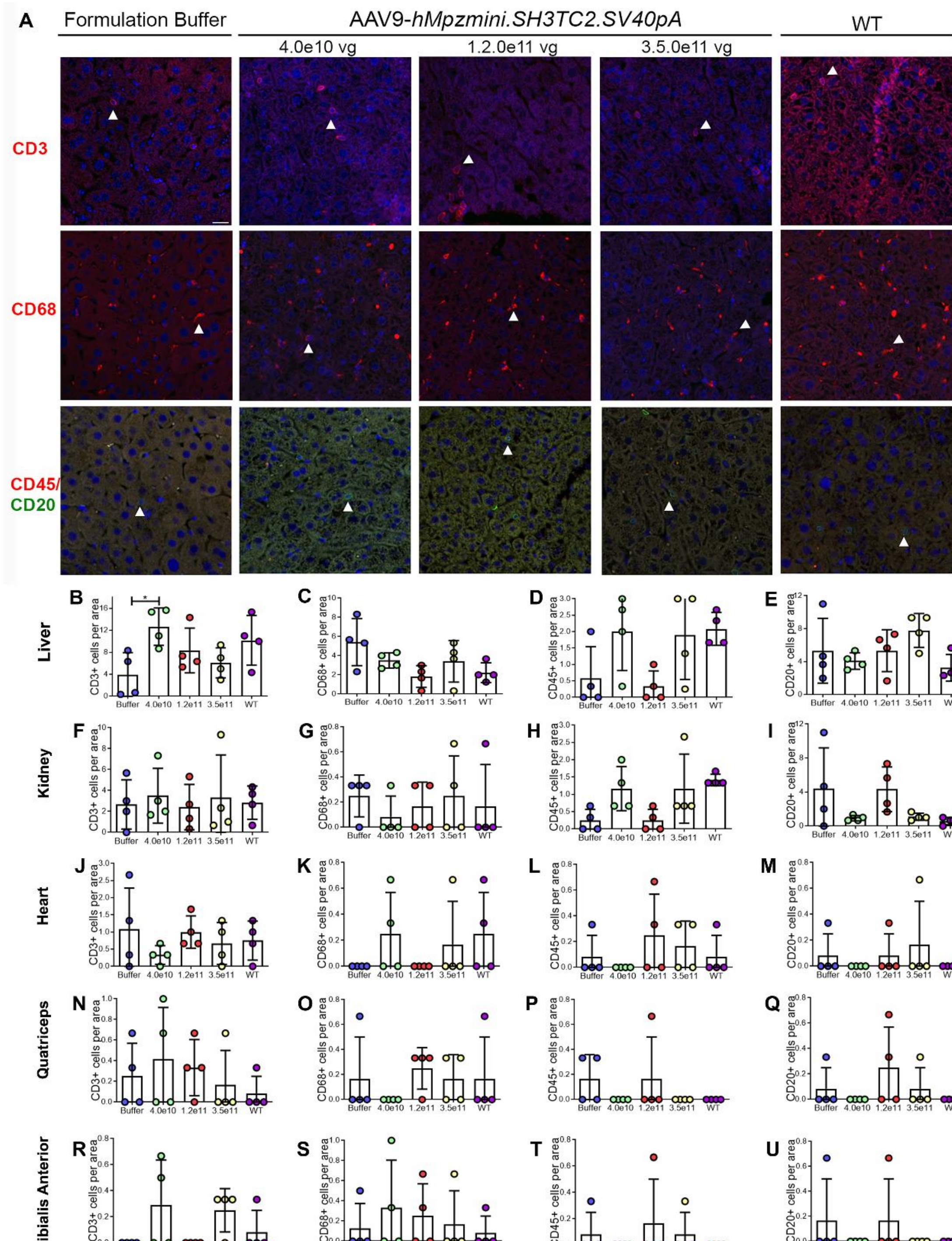
A
Formulation Buffer
AAV9-*hMpzmini.SH3TC2.SV40pA*
WT
4.0e10 vg
1.2.0e11 vg
3.5.0e11 vg
CD3
CD68
CD45/
CD20
B
C
D
E
Liver
F
G
H
I
Kidney
J
K
L
M
Heart
N
O
P
Q
Quatriceps
R
S
T
U
Tibialis Anterior
CD3+ cells per area
CD68+ cells per area
CD45+ cells per area
CD20+ cells per area
Buffer
4.0e10
1.2e11
3.5e11
WT

Fig. S5: Assessment of possible inflammation in the liver of treated *Sh3tc2*$^{-/-}$ mice 8 weeks post injection. A: Representative images of liver sections from *Sh3tc2*$^{-/-}$ mice treated with low, mid, or high vector doses, or with buffer, and from WT mice, immunostained for CD3 (red), CD68 (red), or CD45 (red) and CD20 (green), as indicated. CD+ cells are pointed by a white arrowhead. There is no apparent increase in the numbers of CD+ cells in liver sections from *Sh3tc2*$^{-/-}$ mice regardless of treatment condition, including buffer, compared to WT nerves**. B-F:** Counts of different inflammatory cells per area visualized in sections from different peripheral organs from all treatment groups compared to buffer treated and WT mice (n=4 mice per group). Results were also compared to WT mice of the same age. Diagrams show the results of CD+ cell counts as indicated, in the liver, kidney, heart, quadriceps and tibialis anterior muscles, as indicated. There is no significant difference across groups for CD3+, CD20+, CD45+ or CD68+ cell counts in any of the organs examined (the increased CD3+ cells in the liver of low dose compared to non-injected mice is not consistent in other dose groups). (One-way ANOVA and Tukey's post hoc test, *: $p<0.05$). Scale bars: 20 μm.

Fig. S6

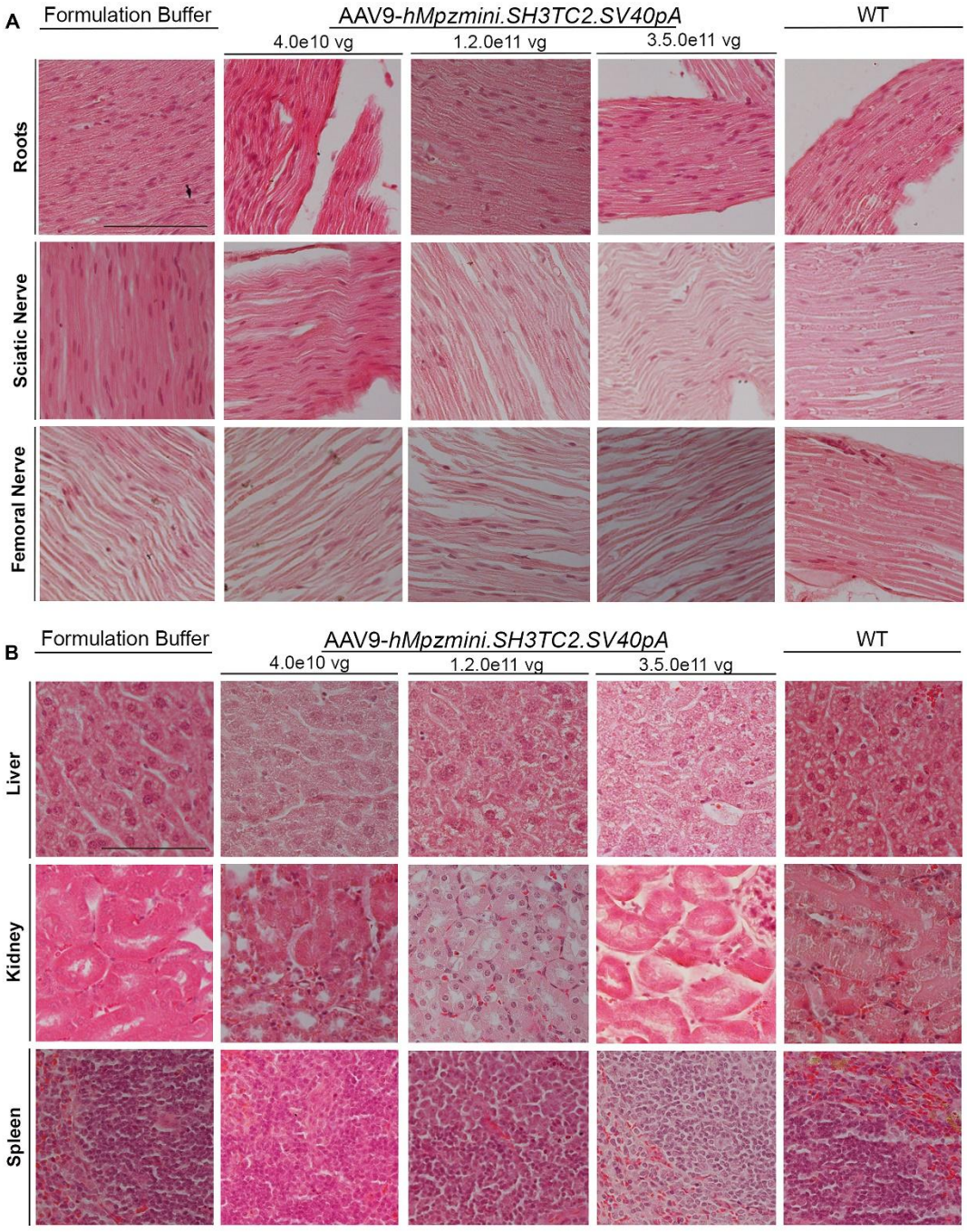
A
Formulation Buffer
AAV9-hMpzmini.SH3TC2.SV40pA
4.0e10 vg
1.2.0e11 vg
3.5.0e11 vg
WT
Roots
Sciatic Nerve
Femoral Nerve
B
Formulation Buffer
AAV9-hMpzmini.SH3TC2.SV40pA
4.0e10 vg
1.2.0e11 vg
3.5.0e11 vg
WT
Liver
Kidney
Spleen

Fig. S6: Preserved neural and peripheral organ tissue integrity in treated mice. Representative images of haematoxylin- and eosin-stained neural tissue sections (A) or peripheral organ sections (B) from Sh3tc2-/-mice, 8 weeks post injection either with the therapeutic vector at the low, mid or high dose, or with buffer alone, and from WT control mice, as indicated. Anterior lumbar spinal roots, sciatic nerves and femoral nerves show no apparent findings of impaired tissue integrity, axon pathology, or inflammation. Likewise, there are no apparent findings of impaired tissue integrity in the liver, kidney or spleen. Scale bars: 50 μm.

Fig. S7

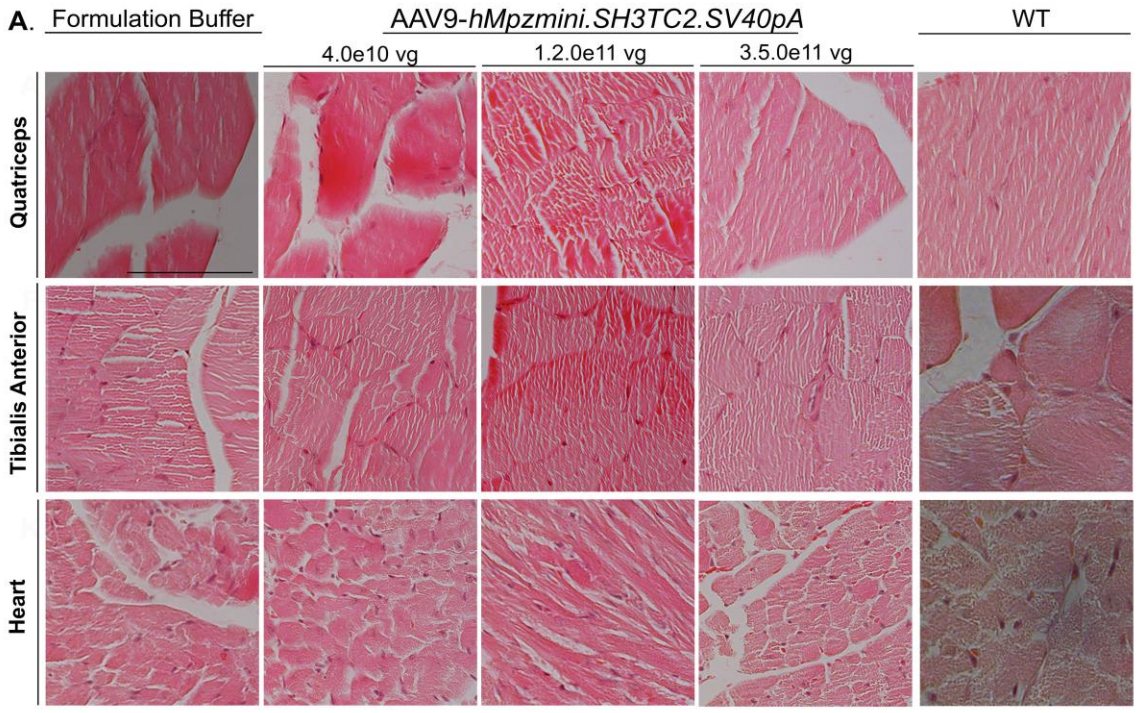

Fig. S7: Lack of tissue toxicity after treatment. Representative images of haematoxylin- and eosin-stained peripheral organ tissue sections including the quadriceps muscle, tibialis anterior muscle, and the heart from *Sh3tc2*$^{-/-}$ mice, 8 weeks post injection with the therapeutic vector at the low, mid or high dose, or with buffer alone, as indicated. There are no apparent findings of impaired tissue integrity or inflammation. Scale bars: 50 μm.

Fig.S8

Fig. S8: Heatmaps of all proteins identified in TA muscle across the different condition. See the photos of the heatmaps at: https://cingaccy-my.sharepoint.com/:f:/g/personal/elenag_cing_ac_cy/EjkTqs5_k8ZCvpGiihoDTEkBoASTF3KzepChA2tgQW3SVw?e=DvWliM